PAPER

Quantum chaos in strong field ionization of hydrogen

IOP Publishing Journal of Physics B: Atomic, Molecular and Optical Physics
J. Phys. B: At. Mol. Opt. Phys. **52** (2019) 225002 (10pp) https://doi.org/10.1088/1361-6455/ab46f1

Quantum chaos in strong field ionization of hydrogen

I A Ivanov[1], **Chang Hee Nam**[1,2] **and Kyung Taec Kim**[1,2]

[1] Center for Relativistic Laser Science, Institute for Basic Science, Gwangju 61005, Republic of Korea
[2] Department of Physics and Photon Science, GIST, Gwangju 61005, Republic of Korea

E-mail: igorivanov@ibs.re.kr

Received 13 June 2019, revised 5 September 2019
Accepted for publication 23 September 2019
Published 22 October 2019

Abstract

We present a study of quantum chaos in the strong field ionization of hydrogen atoms. We use the Bohmian approach to quantum mechanics which allows us to use classical tools such as the Lyapunov exponents to characterize chaotic dynamics. We consider the hydrogen atom in a monochromatic electromagnetic field for the tunneling and intermediate regimes of ionization (corresponding to the values $\gamma \sim 1$ of the Keldysh parameter). We show that with increasing frequency the quantum dynamics of this system becomes increasingly chaotic.

Keywords: quantum chaos, strong field ionization, tunneling ionization

(Some figures may appear in colour only in the online journal)

1. Introduction

It is a well-known feature of the behavior of deterministic systems that they often exhibit extreme sensitivity to small variations of the initial conditions of evolution or to small variations of the parameters of the system (such as the parameters of the Hamiltonian). This property receives the name of chaos [1, 2]. One way to quantify the degree of chaos in classical mechanics is by computing the Lyapunov characteristic exponents (LCE). In particular, the so-called maximal Lyapunov characteristic exponent (MLCE) describes the rate of separation in the time of two orbits starting from arbitrary close initial points. The positivity of the MLCE usually implies the chaotic behavior of the classical system, provided the motion is restricted to a compact region of the phase space.

In quantum mechanics (QM) the situation is different. For a quantum system one cannot define chaotic behavior by looking at the sensitivity of the quantum time evolution with respect to the small variations of the initial state vector. Because of the unitarity of the quantum evolution, the norm of the difference of the two state vectors evolving under the same Hamiltonian is preserved in time. To define quantum chaotic behavior one can study instead the sensitivity of the quantum evolution with respect to the small variations of the parameters of the Hamiltonian [3] or the statistical properties of the spectrum of the system [4–6]. The latter approach has deep implications for the most fundamental questions of statistical physics, in particular, the question of how a quantum system prepared in a nonequilibrium initial state can eventually return to thermal equilibrium. In the framework of the picture of quantum chaos relying on the statistical properties of the spectrum of the system, the typical eigenstate of a chaotic system is a random superposition of integrable states in a narrow energy shell [7]. This fact, and the so-called eigenstate thermalization hypothesis (ETH) [7–10]—which postulates that for a large class of operators their expectation values vary little among the neighboring eigenstates—allow one to show that the quantum system will eventually reach the state of thermal equilibrium.

Yet another possibility for studying quantum chaos is offered by the so-called Bohmian representation of the QM [11]. The Bohmian mechanics (BM) reproduces exactly all the predictions of the orthodox QM [12]. The BM reintroduces the notion of the trajectory in QM so that the electron's motion can be regarded as following a trajectory determined by a velocity field, which, in turn, is defined by the wavefunction obeying the time-dependent Schrödinger equation (TDSE). The Bohmian view of the QM has received a surge of interest recently, in particular for the description of the strong field ionization of atoms [13–15] and various problems of tunneling ionization (such as the spatial and temporal

characteristics of the ionization process) where the visualization of the ionization dynamics offered by the Bohmian trajectories may prove useful [16–18].

The fact that the BM preserves the notion of trajectories allows us to apply classical tools to study the chaotic behavior of quantum systems. A review work [19] describes applications of the BM for the study of quantum chaos in model systems and shows how the use of the BM allows us to adopt the definition and the measure of the chaotic behavior based on the MLCE.

A relatively simple and tractable example of a realistic system showing quantum chaotic behavior is the hydrogen atom in external fields. That this system can exhibit quantum chaos has been known for some time. It was shown on the basis of the statistical analysis of the eigenvalue distribution [4] that hydrogen atoms in static electric and magnetic fields show quantum chaos. A hydrogen atom in an AC electromagnetic field was considered using semi-classical methods [20]. It was found in this work that chaos occurs for the electric field strength exceeding a certain critical value which grows with decreasing frequency. A truncated N-level quantum model of a hydrogen atom exposed to a monochromatic electromagnetic field was considered in [21]. Quantum chaos in this work was studied in the framework of the BM, using the MLCE to characterize the degree of chaos present in the problem. The ionization regime studied in this paper corresponded to the values $\gamma \gg 1$ of the so-called Keldysh parameter $\gamma = \omega\sqrt{2I_p}/E_0$ [22, 23] defined via the ionization potential I_p of the target atom, and the frequency ω and strength E_0 of the electromagnetic field (atomic units are used in the paper unless otherwise specified).

In the present work we use the Bohmian mechanics to study quantum chaos for a hydrogen atom in a linearly polarized monochromatic electric field. We consider the so-called tunneling and intermediate ionization regimes. Within the premise of the Keldysh theory [22] these regimes correspond to the values $\gamma \sim 1$ of the Keldysh parameter. This regime of ionization is of interest as it is known that the tunneling process can be considerably affected by chaos [4, 24–27], which leads to modifications of the usual Keldysh picture of tunneling ionization [20]. We employ a fully *ab initio* model of the hydrogen atom, basing the study of the Bohmian trajectories on the three-dimensional time-dependent Schrödinger equation (TDSE).

2. Theory

For the reader's convenience we begin this section with a brief summary of the basis of the Bohmian approach to quantum mechanics [11]. Substituting the polar form of the wave function of a system $\Psi(\boldsymbol{r}, t) = R(\boldsymbol{r}, t)\exp\{iS(\boldsymbol{r}, t)\}$ with $R(\boldsymbol{r}, t) = |\Psi(\boldsymbol{r}, t)|$ and $S(\boldsymbol{r}, t) = \arg(\Psi(\boldsymbol{r}, t))$ into the the TDSE, describing the evolution of an atomic system in the presence of an external electric field:

$$i\frac{\partial\Psi(\boldsymbol{r}, t)}{\partial t} = -\frac{1}{2}\Delta\Psi(\boldsymbol{r}, t) + V(\boldsymbol{r}, t)\Psi(\boldsymbol{r}, t), \tag{1}$$

with $V(\boldsymbol{r}, t) = -\frac{1}{r} + E(t)\hat{\boldsymbol{z}}\cdot\boldsymbol{r}$ (we use the length gauge to describe atom–field interaction and the electric field is assumed to be linearly polarized along the $z-$ axis); taking real and imaginary parts, one obtains:

$$\frac{\partial S(\boldsymbol{r}, t)}{\partial t} + \frac{1}{2}\left(\frac{\partial S(\boldsymbol{r}, t)}{\partial \boldsymbol{r}}\right)^2 + V_Q(\boldsymbol{r}, t) = 0 \tag{2}$$

$$\frac{\partial R^2(\boldsymbol{r}, t)}{\partial t} + \nabla\cdot(\boldsymbol{v}(\boldsymbol{r}, t)R^2(\boldsymbol{r}, t)) = 0 \tag{3}$$

where the quantum potential $V_Q(\boldsymbol{r}, t)$ and the velocity field $\boldsymbol{v}(\boldsymbol{r}, t)$ are defined as:

$$V_Q(\boldsymbol{r}, t) = V(\boldsymbol{r}, t) - \frac{1}{2}\frac{\Delta R(\boldsymbol{r}, t)}{R(\boldsymbol{r}, t)}, \tag{4}$$

and

$$\boldsymbol{v}(\boldsymbol{r}, t) = \nabla S(\boldsymbol{r}, t). \tag{5}$$

Bohmian interpretation assumes that the tangent curves of the vector field (5) are the trajectories (the so-called Bohmian trajectories) for an ensemble of particles. At the initial moment of time $t = 0$ the coordinates of the particles constituting the ensemble are distributed according to the $R^2(\boldsymbol{r}, 0)$ rule of QM. The difference between the Bohmian and the orthodox interpretations of QM is that the Bohmian approach assumes that the statistical nature of the predictions is solely due to the fact that we deal with a statistical ensemble of particles. In this respect the Bohmian approach to quantum mechanics looks very much like classical statistical mechanics, with the only difference that particles are driven by the quantum potential (4), which, in turn, is linked to the wave-function evolving according to the TDSE.

Initial velocities of the particles of the ensemble are given by equation (5) evaluated at $t = 0$. Equation (2) is the Hamilton–Jacobi equation for the system described by the quantum potential (4). The Bohmian trajectories, therefore, are solutions to Newton's equations of motion, equivalent to the Hamilton–Jacobi equation (2) with the initial conditions specified above. In practice, it is easier to find the trajectories by integrating equation (5) along each trajectory, provided that the velocity field $\boldsymbol{v}(\boldsymbol{r}, t)$ is known as a function of coordinates and time. To find the velocity field we have to solve the TDSE.

We consider below a hydrogen atom in the field of a monochromatic laser pulse $E(t) = E_0\cos\omega t$. The initial state of the system is the ground state. We solve the fully three-dimensional TDSE employing the procedure described in detail in [28]. We give, therefore, only the most essential details of this procedure.

The solution of the TDSE is represented as a series in spherical harmonics:

$$\Psi(\boldsymbol{r}, t) = \sum_{l=0}^{L_{\max}} f_l(r, t)Y_{l0}(\theta). \tag{6}$$

The radial part of the TDSE is discretized on the grid with the step-size $\delta r = 0.025$ a.u. in a box of size $R_{\max} = 1200$ a.u. The number of partial waves one needs to use in equation (6) to achieve convergence depends on the field parameters and increases quickly with decreasing frequency. For the lowest field frequency $\omega = 0.03$ a.u. and for the field intensity of $10^{14}\,\mathrm{W\,cm^{-2}}$ ($E_0 = 0.053\,4$ a.u.) we consider below, it is enough to use $L_{\max} = 80$ in equation (6) to achieve convergence.

Using the numerically computed solution to the TDSE and equation (5), we determine the velocity field as a function of coordinates and time. Since the wave-function in our approach is defined on a spatial grid, we obtain the velocity field at the the grid points. The velocity field at other points was found by means of the Lagrange interpolation procedure. The velocity field (5) inherits the symmetry with respect to the rotations around the z-axis which the TDSE wave-function possesses for the field geometry in our problem. For the initial ground state of the hydrogen atom, all the Bohmian trajectories launched at $t = 0$ have zero velocities. It is a well-known feature of the Bohmian QM [11] that the velocity field in a state described by a real wave-function is zero. The physical possibility of this state of motion in the Bohmian picture is due to the fact that the force corresponding to the quantum potential (4) vanishes in this case allowing the particles to stay at rest. A trajectory with the initial conditions $\boldsymbol{r}(0) = \boldsymbol{r}_0$ will remain in the plane formed by the vectors $\boldsymbol{r}_0$ and $\hat{\boldsymbol{z}}$ in the course of evolution. It is sufficient, therefore, to compute the velocity field in any plane containing a z-axis. We choose the (x, z)-plane for this purpose. The evolution of the trajectories in time is found then by integrating numerically the system of differential equations $\frac{d\boldsymbol{r}}{dt} = \boldsymbol{v}(\boldsymbol{r}, t)$ with the velocity field (5) and initial conditions $x(0) = x_0$, $z(0) = z_0$ in the (x, z)-plane.

3. Results

Depending on the subsequent evolution we may divide the Bohmian trajectories in our problem into two classes: unbound trajectories corresponding to ionized electrons and the trajectories remaining in the compact region of the configuration space. This division was used in the literature [16, 18] to study the dynamics of the tunneling ionization. For the frequencies and the field strengths we consider in this work we illustrate this separation of trajectories into bound and unbound classes in figure 1. The trajectories were launched at $t = 0$ from different (x_0, z_0) points in the (x, z)-plane and we followed their evolution in the interval of time $(0, T_1)$, where $T_1 = 4T$ and the $T = 2\pi/\omega$ is the duration of the optical cycles (o.c.) corresponding to the particular frequency ω. The criteria of ionization we imposed were that the trajectories for which the distance to the center exceeds the value $d_0 = 20$ a.u. at least once during the evolution are considered as unbound. The particular value of d_0 is not very important: figure 1 would not change appreciably had we used the value $d_0 = 10$ a.u.

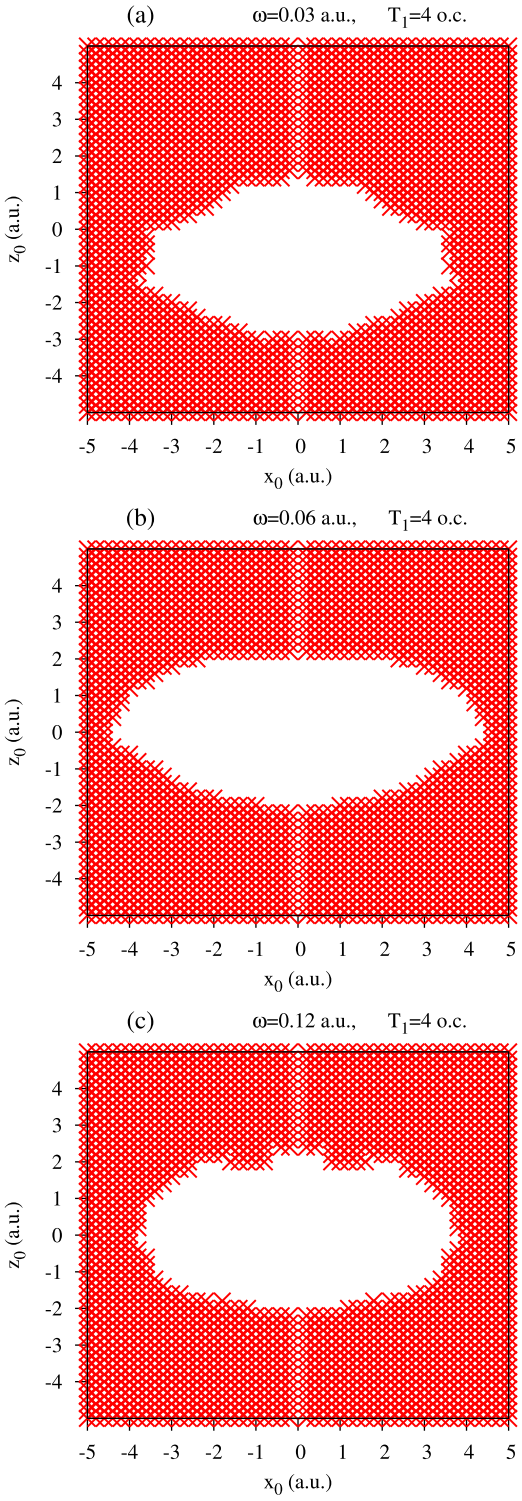

Figure 1. The dependence of the type of electron trajectory on the initial coordinates in the (x, z)-plane for a pulse with peak strength $E_0 = 0.053\,4$ a.u. and total duration $T_1 = 4$ o.c. The initial values x_0, z_0 corresponding to the ionized trajectories are in the (red) filled area.

The aim of the present work is to apply the tools used to study classical chaos, such as the LCE, to Bohmian trajectories. A necessary condition for this to be done is the bound character of motion. This condition is imposed to exclude trivial cases, e.g., the system of differential equations

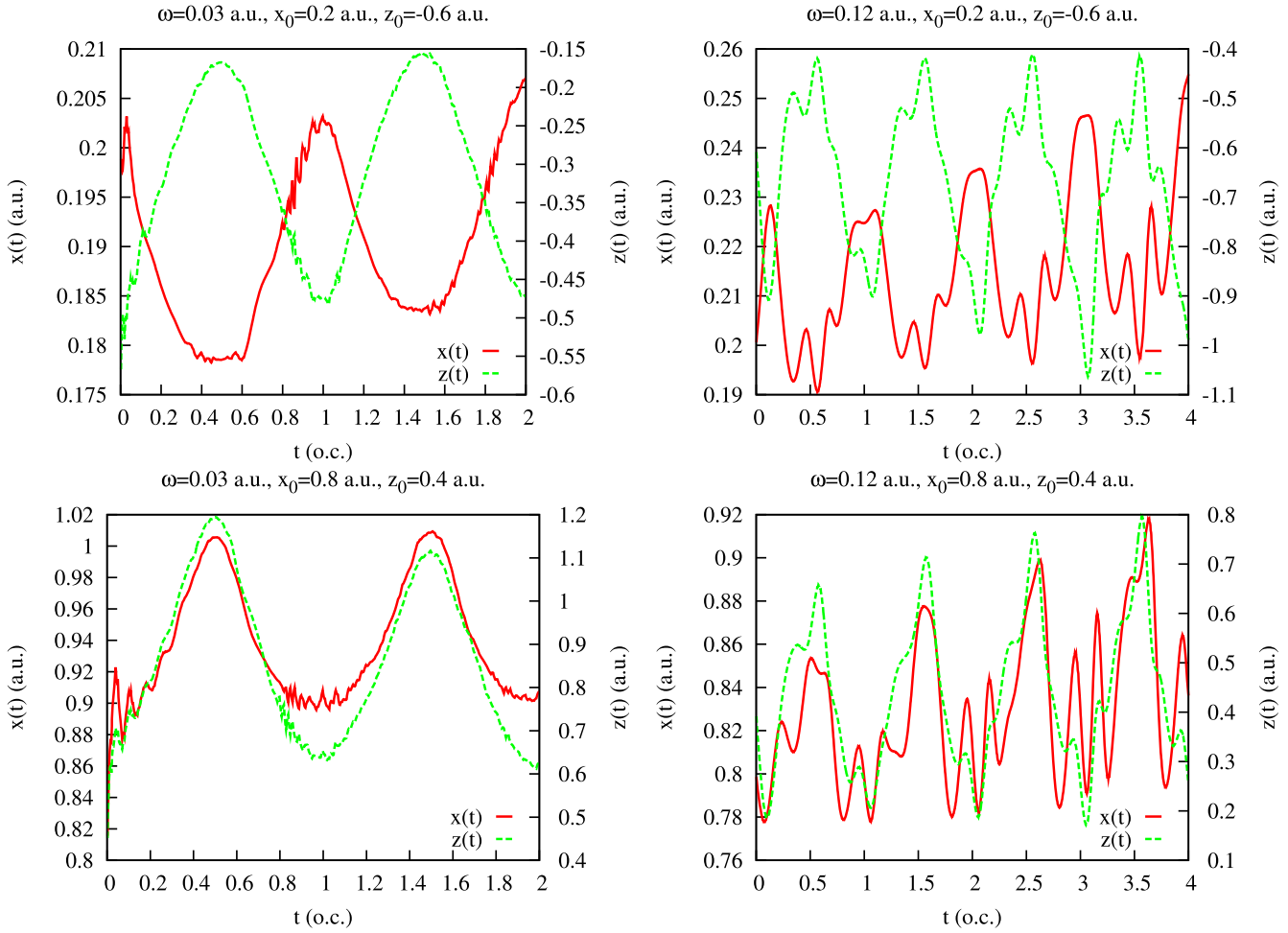

Figure 2. Bohmian trajectories ($x(t)$, $z(t)$) corresponding to the finite motion for difference frequencies ω and different initial conditions (x_0, z_0).

$\dot{x} = ax$, $\dot{z} = bz$ with $a > 0$, $b \neq a$ for which solutions do not exhibit chaotic behavior, but the trajectories exponentially diverge in time. Although there are approaches [29] allowing us to use tools such as the LCE or Poincare maps to characterize the unbound classical chaotic motion, they are less transparent. In the present work we concentrate, therefore, on the Bohmian trajectories corresponding to the finite bounded motion of electrons on the interval of time we consider. Figure 1 shows that, in agreement with the results obtained in [16], these are the trajectories originating inside certain areas in the (x, z)-plane. A study of these trajectories is presented below.

3.1. Bound Bohmian trajectories

We show in figure 2 examples of the bound trajectories ($x(t)$, $z(t)$) for different frequencies and a peak field strength $E_0 = 0.053\,4$ a.u. of the driving field. One can see that for the low frequency of $\omega = 0.03$ a.u. the Bohmian trajectories are (almost) smooth and regular curves. The trajectories for the higher frequency $\omega = 0.12$ a.u. become more irregular, behavior which is commonly associated with the advent of chaos. This observation suggests that with the increasing frequency of the driving electric field the system becomes increasingly chaotic.

As yet another illustration of the plausibility of this statement we show in figures 3–5 the integral curves (i.e. the curves in the (x, z)-plane given parametrically by the equations $x = x(t)$, $z = z(t)$, where $x(t)$, $z(t)$ are solutions to equation (5)). For each frequency ω shown in the figures we consider the interval of time $(0, 4T)$, where $T = 2\pi/\omega$ is the optical cycle duration.

One can see that with increasing frequency the integral curves of equation (5) fill progressively larger areas of the (x, z)-plane. This observation supports the assertion we made above that with increasing frequency the behavior of the system becomes progressively more chaotic. Indeed, the intuitive idea of chaotic behavior is that in the case of completely chaotic dynamics, the integral curve must pass with an equal probability in the vicinity of any point of the available configuration space. It should be noted that for each frequency in figure 5 the total time interval in which the motion is considered is four optical cycles of the corresponding frequency. These intervals are, therefore, different for different frequencies. In particular, the total time interval for the frequency $\omega = 0.12$ a.u. is four times smaller than the total time interval for the frequency $\omega = 0.03$ a.u. Had we used the

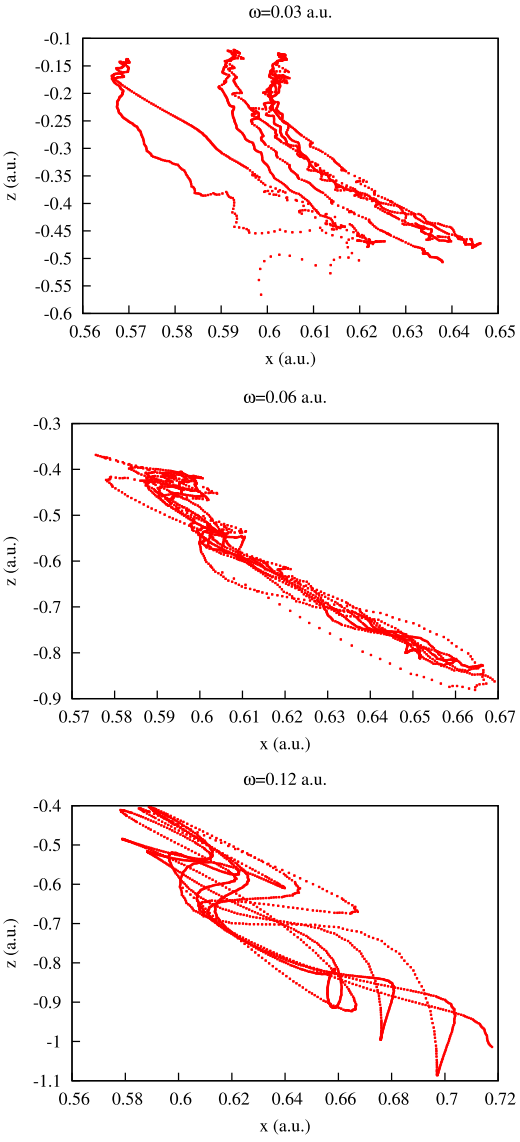

Figure 3. The integral curve for the Bohmian trajectory $(x(t), z(t))$ for $t \in (0, 4T)$ ($T = 2\pi/\omega$ is the optical cycle corresponding to the frequency ω) for different driving frequencies. The initial values of the coordinates: $x_0 = 0.6$ a.u., $z_0 = -0.6$ a.u.

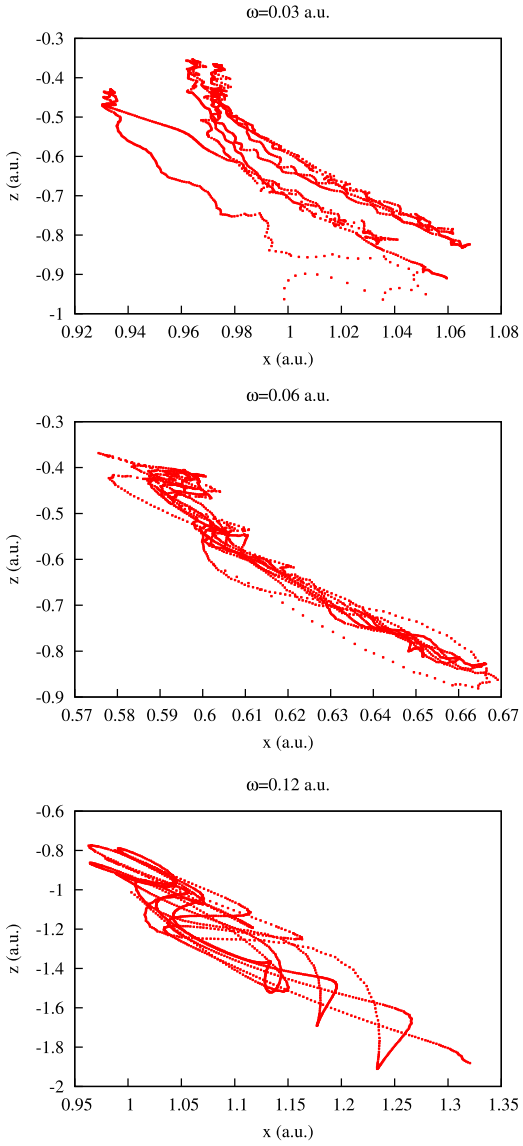

Figure 4. The integral curve for the Bohmian trajectory $(x(t), z(t))$ for $t \in (0, 4T)$ ($T = 2\pi/\omega$ is the optical cycle corresponding to the frequency ω) for different driving frequencies. The initial values of the coordinates: $x_0 = 1$ a.u., $z_0 = -1$ a.u.

interval of equal length in both cases we would get, of course, a still more densely filled area in the (x, z)-plane for the frequency $\omega = 0.12$.

A more precise quantitative measure of the chaotic behavior is provided by the Lyapunov critical exponents. In particular if the MLCE is positive the system is said to be chaotic [30]. Estimates of the MLCEs for different frequencies of the driving electric field are presented below.

3.2. Estimate of the MLCE

The MLCE for an autonomous system of differential equations (having in mind the system (5) vector $\boldsymbol{u}$ in the equation below is a two-component vector with the components x, z, and $\boldsymbol{v}$ is the vector field):

$$\dot{\boldsymbol{u}} = \boldsymbol{v}(\boldsymbol{u}) \tag{7}$$

can be defined as [30]:

$$\lambda = \lim_{\substack{t\to\infty \\ d_0\to 0}} \lambda(t), \tag{8}$$

where

$$\lambda(t) = \frac{1}{t} \ln \frac{d(t)}{d_0}, \tag{9}$$

and $d(t)$ is the distance $d(t) = |\boldsymbol{u}_r(t) - \boldsymbol{u}_s(t)|$ between two trajectories ($\boldsymbol{u}_r(t)$ is the reference trajectory and $\boldsymbol{u}_s(t)$ is the shadow one), initially separated by the distance d_0. In practice the double limit in equation (9) is not easy to implement. We use, therefore, an equivalent procedure described, e.g., in [19].

We add to system (7) a system of variational linearized equations [19] which are obtained from equation (7) for small variations $\xi_x(t)$ and $\xi_z(t)$ around the reference trajectory $x(t)$, z

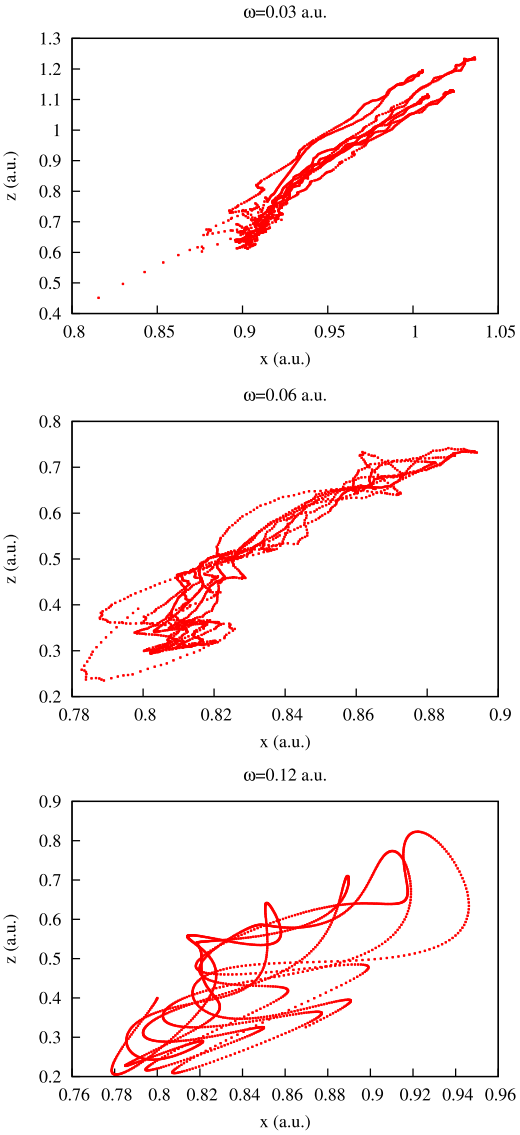

Figure 5. The integral curve for the Bohmian trajectory $(x(t), z(t))$ for $t \in (0, 4T)$ ($T = 2\pi/\omega$ is the optical cycle corresponding to the frequency ω) for different driving frequencies. The initial values of the coordinates: $x_0 = 0.8$ a.u., $z_0 = 0.4$ a.u.

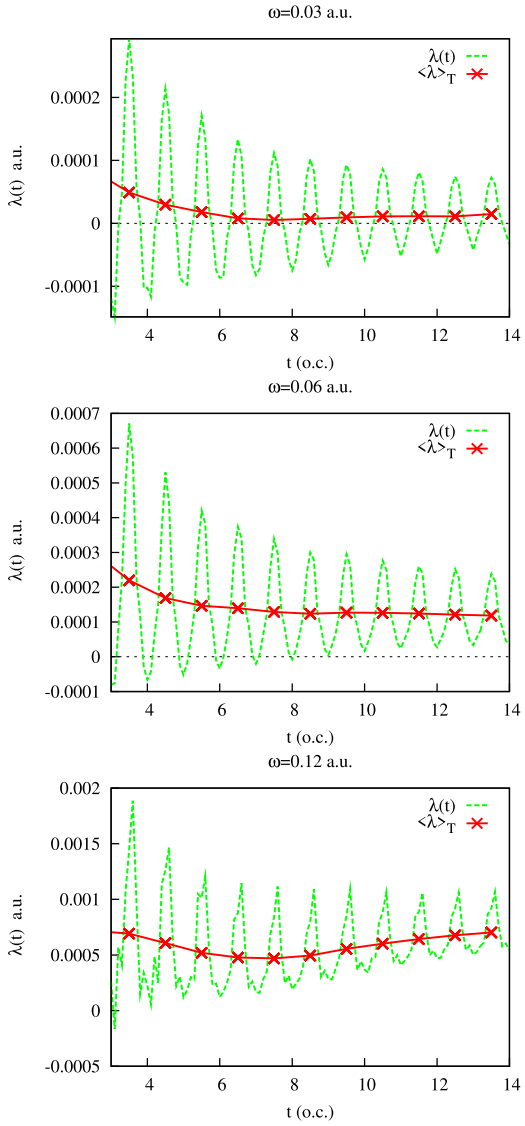

Figure 6. Dashed (green) line: calculation of MLCE according to equation (11) for the Bohmian trajectory with initial values $x_0 = 0.8$ a.u., $z_0 = 0.4$ a.u. Solid (red): cycle average of equation (11).

(t):

$$\frac{d\boldsymbol{\xi}}{dt} = (\boldsymbol{\xi} \cdot \nabla_{\boldsymbol{u}})\boldsymbol{v}(\boldsymbol{u}). \tag{10}$$

Equation (10) is to be solved together with equation (7). The initial conditions for $\boldsymbol{\xi}$ can be arbitrary nonzero values. The MLCE can be obtained as [19]:

$$\lambda = \lim_{t\to\infty} \lambda(t) = \lim_{t\to\infty} \frac{1}{t} \ln \frac{|\boldsymbol{\xi}(t)|}{|\boldsymbol{\xi}(0)|}, \tag{11}$$

where $|\boldsymbol{\xi}(t)|$ is the Euclidean norm of the vector $\boldsymbol{\xi}(t)$. The advantage of this prescription for the calculation of the MLCE compared to definition (8) is that we need not worry about taking the double limit, which may be troublesome in a numerical calculation. The system is chaotic if $\lambda > 0$. Definition (8) is usually applied to the autonomous system of ODE. System (5) is not autonomous, since the velocity field depends on time. It can be shown [19] that equation (11) can still be used to define the MLCE in the nonautonomous case.

Application of this procedure is illustrated in figure 6. As an example we use the trajectory with the initial conditions $x_0 = 0.8$ a.u., $z_0 = 0.4$ a.u. One can see that the calculations of the MLCE following prescription (11) produce oscillating curves with a slowly decaying amplitude of oscillations. The fact that $\lambda(t)$ still does not reach the limiting value even for times as long as 14 optical cycles is not surprising: MLCEs are known to converge notoriously slowly to the limiting values [19]. To achieve good accuracy in determining the MLCEs one usually has to follow trajectories for a very long time. While such calculations may be feasible for some model quantum systems, the interval of time over which we can follow the trajectories in our problem is limited by the constraints of the numerical character. Solving the TDSE for long time intervals (especially for frequencies as low as $\omega = 0.03$ a.u. which we consider below) is a very demanding

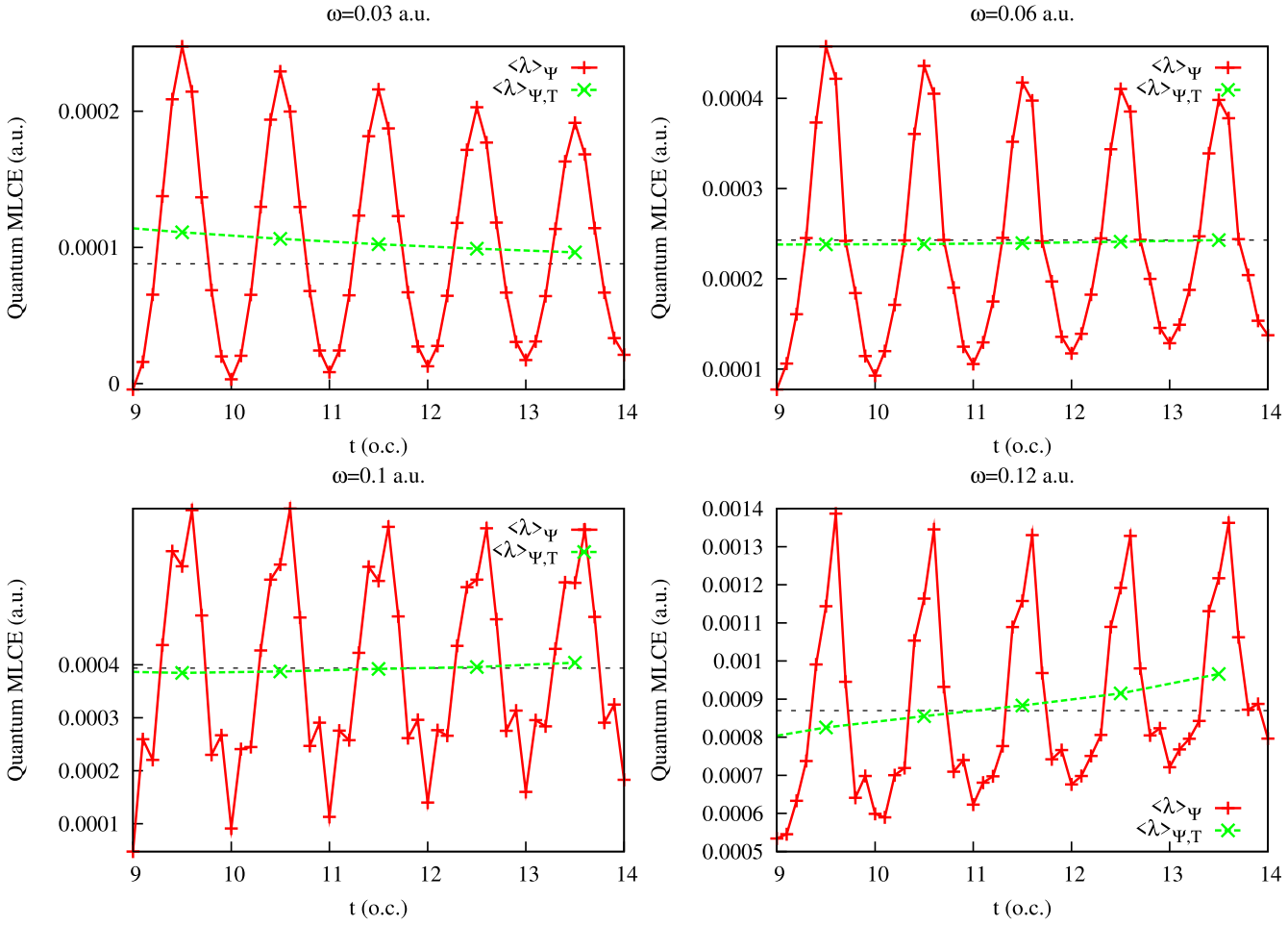

Figure 7. The quantum MLCE for different frequencies of the driving field. Solid (red) line and (red) crosses: $\langle\lambda\rangle_{\Psi}(t)$—quantum averaged finite time MLCE. Long dashed (green) line: $\langle\lambda\rangle_{\Psi,T}$—cycle average (12). (Black) short dashed: large-t limit predicted by the ϵ-algorithm.

Table 1. Global quantum MLCE obtained by using the ϵ-algorithm and the convergence acceleration method (12).

ω (a.u.)	ϵ-algorithm	Equation (12)
0.03	8.8×10^{-5}	9.6×10^{-5}
0.06	2.42×10^{-4}	2.38×10^{-4}
0.1	3.93×10^{-4}	4.04×10^{-4}
0.12	8.7×10^{-4}	9.6×10^{-4}

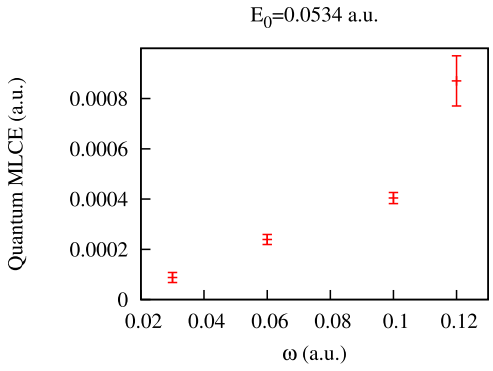

Figure 8. Estimates of the global quantum MLCE for different frequencies of electromagnetic field.

computational task, even in the case of the hydrogen atom we consider presently.

To determine the MLCE in our calculation we solve the TDSE on the time interval (0, 14T) for each frequency. For this time-interval we can calculate the time-dependent wavefunction, and consequently the vector field (5) accurately with a reasonable computational cost. The procedure which we have described gives us, therefore, $\lambda(t)$ on a finite time interval. In this way we obtain the so-called finite [31] MLCE, which can provide useful information about the stability of the trajectories at finite time intervals [31]. We are interested, however, in the so-called global MLCE [31] corresponding to the infinite time limit in equations (9) and (11). The question regarding the extent to which we may hope to gain an insight into the limiting global MLCE using our finite time data is addressed below.

3.3. Global MLCE

As we noted before, the finite MLCEs in figure 6 are oscillating functions of time with a slowly decaying amplitude of oscillations. While for the time intervals shown in figure 6 we are certainly far from the time values where MLCE attains the limiting value, we can nevertheless try to extract some

information about these limiting values from the finite time data. The expectations that this task may be feasible are based on the observation that for each frequency the finite MLCE $\lambda(t)$ in figure 6 exhibits oscillations with a period of approximately one optical cycle. One can, therefore, attempt to accelerate the convergence of the $\lambda(t)$ by introducing a sequence $\langle\lambda\rangle_N$—the cycle average of $\lambda(t)$:

$$\langle\lambda\rangle_N = \frac{1}{T}\int_{NT}^{(N+1)T} \lambda(t)\, dt. \tag{12}$$

It is easy to see that if $\lambda(t)$ behaves asymptotically as:

$$\lambda(t) \sim \lambda_\infty + f(t)\cos(\omega t + \delta), \tag{13}$$

where $f(t)$ decays monotonously for $t \to \infty$, then if $f(t)$ varies slowly in the interval of one optical cycle (more precisely if $|f'(t)/f(t)| \ll \omega$ on this interval), then the cycle average of the function $\lambda(t)$ given by (13) will converge to the same limit λ_∞ faster than the original $\lambda(t)$. We can expect that the decay of the oscillations of the $\lambda(t)$ in our case will be due to the contribution of the second LCE λ_2. Then the behavior of $\lambda(t)$ in our problem can be roughly mimicked by equation (13) with $f(t)$ decaying with time as $e^{-\Gamma t}$ where $\Gamma \approx \lambda - \lambda_2$, and λ and λ_2 are, correspondingly, the MLCE and the smaller second Lyapunov exponent. We can hope, therefore, that our convergence acceleration method based on the cycle average will work if $|\lambda - \lambda_2| \ll \omega$. That this reasoning is at least partly correct can be seen in figure 6, where the cycle-averaged sequences are shown for different frequencies ω.

One can see that cycle averaging indeed removes oscillations almost completely and allows us to make a fairly accurate estimate of the global infinite time MLCE for this trajectory in the cases of $\omega = 0.03$ a.u. and $\omega = 0.06$ a.u. For $\omega = 0.12$ a.u. the global MLCE for this trajectory apparently has a value larger than 10^{-3} a.u., and the criterion $|\lambda - \lambda_2| \ll \omega$ for the validity of the convergence acceleration procedure (12) is, probably, not fulfilled. Nevertheless, figure 6 shows that even in this case we can make at least a rough estimate of the infinite time MLCE.

In the next section, we will describe use of the convergence acceleration procedure (12) for the calculations of the maximum Lyapunov exponents for different frequencies of the driving field. To confirm the results of the averaging procedure we will also use a more general technique of acceleration of convergence: the so-called ϵ-algorithm [32, 33]. This algorithm is a certain nonlinear transformation of the original sequence, such that the transformed sequence converges to the same limit but faster than the original one. In deriving our convergence acceleration procedure (12) we used a tentative formula for the asymptotic behavior of $\lambda(t)$ suggested by the numerical calculation. The power of the ϵ-algorithm is that it does not rely on particular assumptions about the asymptotic behavior of a sequence. This algorithm works well for sequences with different asymptotic behaviors [32, 33] and is, therefore, more general than the averaging procedure (12). Below we will use both techniques to find the infinite time limits of the MLCE, and the difference between the results of the two methods will provide us with an estimate of the numerical error. In the next section we describe the application of this strategy for the calculations of the so-called quantum global MLCE [21].

3.4. Quantum global MLCE

We described above the application of the convergence acceleration technique based on cycle average using a single Bohmian trajectory as an example. We are interested, however, in a more general characterization of chaos which would not depend on a particular set of initial conditions. Such a characterization, the so-called quantum global MLCE, is given by a quantum mechanical average of the global MLCE for different Bohmian trajectories [21]:

$$\langle\lambda\rangle_\Psi = \int |\Psi(\boldsymbol{r}_0, 0)|^2 \lambda(\boldsymbol{r}_0)\, d\boldsymbol{r}, \tag{14}$$

where $\Psi(\boldsymbol{r}, 0)$ is the wave-function of the initial state (the ground state of the hydrogen atom in our problem) and $\lambda(\boldsymbol{r}_0)$ is the maximum Lyapunov exponent for a Bohmian trajectory originating at $\boldsymbol{r} = \boldsymbol{r}_0$ at $t = 0$. In equation (14) we use the notation $\lambda(\boldsymbol{r}_0)$ to emphasize the dependence on the initial conditions. We also employ in equation (14) the notation $\langle\lambda\rangle_\Psi$ to emphasize that the averaging is performed over the initial conditions distributed according to the quantum-mechanical probability density. We discussed the calculation of the $\lambda(\boldsymbol{r}_0)$ in the previous section using a particular case of $\boldsymbol{r}_0 = (0.8, 0, 0.4)$ a.u. as an example.

To estimate the quantum global MLCE we proceed as follows. We described above the procedure for the calculation of the finite time MLCE $\lambda(\boldsymbol{r}_0, t)$ for a given trajectory. Substituting the finite time MLCE $\lambda(\boldsymbol{r}_0, t)$ in equation (14) we obtain the function $\langle\lambda\rangle_\Psi(t)$—the finite time quantum MLCE. The results are shown in figure 7.

Figure 7 shows that the averaged finite time MLCEs inherit the oscillating character of the nonaveraged $\lambda(\boldsymbol{r}_0)$. By the same reasoning we used above discussing convergence acceleration for $\lambda(\boldsymbol{r}_0, t)$, this fact again makes it plausible to use the convergence acceleration method based on cycle averaging (12) to estimate the infinite time limit. The results of this procedure, as well as the results of the estimate of the infinite time limit obtained using the ϵ-algorithm, are shown in figure 7. These data are also shown in table 1. As one can see, the results of the two convergence acceleration techniques for $\omega = 0.06$ a.u. and $\omega = 0.1$ a.u. agree quite well. Visually, the two methods do not agree so well for the lowest frequency of $\omega = 0.03$ a.u., as compared to the cases of $\omega = 0.06$ a.u. and $\omega = 0.1$ a.u., but this is because the global quantum limiting MLCE for $\omega = 0.03$ a.u. is quite small. We adopt the difference of the two estimates for the global quantum MLCE, obtained by using convergence acceleration techniques based on (12) and the ϵ-algorithm, as an estimate of the absolute error of our results. With this definition, as one can see from the data in table 1, the absolute errors for $\omega = 0.03$ a.u., $\omega = 0.06$ a.u. and $\omega = 0.1$ a.u. can be estimated as 10^{-5} a.u. For the larger frequency $\omega = 0.12$ a.u. the difference of the results given by the two convergence acceleration techniques is larger, and the estimate of the absolute error of our result for this frequency is closer to 10^{-4}

a.u. Our final results for the global quantum MLCE with estimates for the absolute errors obtained as described above are summarized in figure 8.

4. Conclusion

We presented the results of a study of quantum chaos for a hydrogen atom subjected to strong electromagnetic fields with various frequencies. Our study was based on the Bohmian representation of the QM. Computation of the Bohmian trajectories relied on the numerical solution of the fully three-dimensional TDSE. The study of the Bohmian trajectories enabled us to use tools such as the Lyapunov exponents, in particular the MLCE, as a quantitative measure of the chaotic behavior of the system.

A very interesting question is whether looking at the quantum chaos from the point of view of Bohmian mechanics can be used to distinguish between the Bohmian and the conventional versions of the QM. We share the view [11, 12, 34] that all the empirically testable predictions of the Bohmian and the conventional QM, whenever the latter are unambiguous, should agree. BM and the conventional QM then differ only in the interpretations they offer and the fact that some puzzling features of the conventional QM, such as the postulate of the collapse of the wave-function in the measurement process, find an explanation in the framework of the BM [11]. Therefore, our answer to this question would rather be negative. The interpretation which BM offers can, however, provide us with useful tools, especially when approaches to quantum chaos relying on the conventional QM, such as analysis of the statistical properties of the spectrum of the Hamiltonian are not directly applicable. This is the case for the present time-dependent problem.

The Bohmian trajectories are not very simple objects to handle. To escape the restrictions imposed by the Bell's inequalities [35], which rule out the local modifications of the QM, the Bohmian trajectories must exhibit rather peculiar properties. The intrinsic property of the nonlocality of the QM, as exemplified by the Einstein–Podolsky–Rosen paradox, appears in the Bohmian picture in another guise. Thus, a measurement performed in a place may have an instantaneous effect on the Bohmian trajectory of a particle that can be far away. This fact can be used to steer the trajectories of Bohmian particles [36]. Nevertheless, the Bohmian trajectories can, as we tried to demonstrate, be computed reliably and their study can provide useful information.

The particular calculation of the MLCE we described above proved a rather nontrivial task in the ionization regime we consider. The finite time MLCE are known to converge to their infinite time limiting values extremely slowly. We cannot expect to be able to solve the TDSE accurately for such long time intervals, and this hardly makes it possible to directly attempt to compute the infinite time global MLCE by following the quantum evolution of the system over a long enough time interval. We were able to circumvent this problem by using convergence acceleration techniques. The averaging method based on equation (12), which we devised, and the well-known ϵ-algorithm provided us with estimates for both the MLCE and the expected error for the different frequencies we considered. Our data summarized in figure 8 and table 1 show that following this strategy we were able to achieve a reasonable accuracy in our MLCE estimates. We found that both the qualitative picture of the Bohmian trajectories and quantitative analysis based on the calculation of the MLCEs show that the system becomes increasingly more chaotic with increasing frequency.

Acknowledgments

This work was supported by the Institute for Basic Science under grant number IBS-R012-D1. IAI benefited from useful discussions with A Landsman.

ORCID iDs

I A Ivanov https://orcid.org/0000-0003-3856-1658

References

[1] Gutzwiller M C 1990 *Chaos in Classical and Quantum Mechanics* (Berlin: Springer)
[2] Zaslavsky G M 1985 *Chaos in Dynamic Systems* (New York: Harwood Academic Publishers)
[3] Peres A 1984 *Phys. Rev.* A **30** 1610
[4] Delande D and Zakrewski J 2003 *Phys. Rev.* A **68** 062110
[5] Bohigas O, Giannoni M J and Schmit C 1984 *Phys. Rev. Lett.* **52** 1
[6] Izrailev F 1987 *Phys. Rev. Lett.* **125** 250
[7] Deutsch J M 1991 *Phys. Rev.* A **43** 2046
[8] Srednicki M 1994 *Phys. Rev.* E **50** 888
[9] Rigol V M, Dunjko V and Olshanii M 2008 *Nature* **452** 854
[10] Eisert J, Friesdorf M and Gogolin C 2015 *Nat. Phys.* **11** 124
[11] Bohm D 1952 *Phys. Rev.* **85** 166
[12] Bell J S 1987 *Speakable and Unspeakable in Quantum Mechanics* (Cambridge: Cambridge University Press)
[13] Botheron P and Pons B 2010 *Phys. Rev.* A **82** 021404(R)
[14] Sawada R, Sato T and Ishikawa K L 2014 *Phys. Rev.* A **90** 023404
[15] Wu J, Augstein B B and de Morisson Faria C F 2013 *Phys. Rev.* A **88** 063416
[16] Douguet N and Bartschat K 2018 *Phys. Rev.* A **97** 013402
[17] Zimmermann T, Mishra S, Doran B R, Gordon D F and Landsman A S 2016 *Phys. Rev. Lett.* **116** 233603
[18] Ivanov I A, Nam C H and Kim K T 2017 *Sci. Rep.* **7** 39919
[19] Efthymiopoulos C and Contopoulos G 2006 *J. Phys. A: Math. Gen.* **39** 1819
[20] Krainov V P 2014 *J. Phys.* B **47** 204006
[21] Iacomelli G and Pettini M 1996 *Phys. Lett.* A **212** 29
[22] Keldysh L V 1965 *Sov. Phys. JETP* **20** 1307
[23] Krausz F and Ivanov M 2009 *Rev. Mod. Phys.* **81** 163
[24] Lin W A and Ballentine L E 1990 *Phys. Rev. Lett.* **65** 2927
[25] Grossmann F, Dittrich T, Jung P and Hänggi P 1991 *Phys. Rev. Lett.* **67** 516
[26] Tomsovic S and Ullmo D 1994 *Phys. Rev.* E **50** 145
[27] Leyvraz F and Ullmo D 1996 *J. Phys. A: Math. Gen.* **29** 2529
[28] Ivanov I A 2014 *Phys. Rev.* A **90** 013418
[29] Jung C 1986 *J. Phys. A: Math. Gen.* **19** 1345
[30] Tancredi G, Sánchez A and Roig F 2001 *Astron. J* **121** 1171

[31] Vallejo J C and Sanjuán M A F 2013 *New J. Phys.* **15** 113064
[32] Graves-Morris P R, Roberts D E and Salam A 2000 *J. Comput. Appl. Math.* **122** 51
[33] Weniger E J 1996 *Ann. Phys.* **246** 133
[34] Dürr D, Goldstein S and Zanghì N 1992 *J. Stat. Phys.* **67** 843
[35] Bell J S 1964 *Physics* **1** 195
[36] Xiao Y, Kedem Y, Xu J-S, Li C-F and Guo G-C 2017 *Opt. Express* **25** 14463